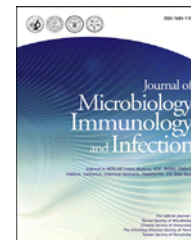


Available online at www.sciencedirect.com

ScienceDirect

journal homepage: www.e-jmii.com

ORIGINAL ARTICLE

Toxic effect of high concentration of sonochemically synthesized polyvinylpyrrolidone-coated silver nanoparticles on *Citrobacter* sp. A1 and *Enterococcus* sp. C1



Chew Ping Lau ^a, Mohd Firdaus Abdul-Wahab ^a,
Jafariah Jaafar ^b, Giek Far Chan ^c, Noor Aini Abdul Rashid ^{a,*}

^a Faculty of Biosciences and Medical Engineering (FBME), Universiti Teknologi Malaysia (UTM), Johor, Malaysia

^b Faculty of Science, Universiti Teknologi Malaysia (UTM), Johor, Malaysia

^c School of Applied Science, Temasek Polytechnic, Singapore

Received 17 February 2015; received in revised form 20 June 2015; accepted 31 August 2015

Available online 9 September 2015

KEYWORDS

Citrobacter sp. A1;
Enterococcus sp. C1;
silver nanoparticles;
tolerance level;
toxic effect

Abstract *Background/Purpose:* Currently, silver nanoparticles (AgNPs) have gained importance in various industrial applications. However, their impact upon release into the environment on microorganisms remains unclear. The aim of this study was to analyze the effect of polyvinylpyrrolidone-capped AgNPs synthesized in this laboratory on two bacterial strains isolated from the environment, Gram-negative *Citrobacter* sp. A1 and Gram-positive *Enterococcus* sp. C1.

Methods: Polyvinylpyrrolidone-capped AgNPs were synthesized by ultrasound-assisted chemical reduction. Characterization of the AgNPs involved UV–visible spectroscopy, Fourier transform infrared spectroscopy, X-ray diffraction, transmission electron microscopy, and energy dispersive X-ray spectroscopy. *Citrobacter* sp. A1 and *Enterococcus* sp. C1 were exposed to varying concentrations of AgNPs, and cell viability was determined. Scanning electron microscopy was performed to evaluate the morphological alteration of both species upon exposure to AgNPs at 1000 mg/L.

Results: The synthesized AgNPs were spherical in shape, with an average particle size of 15 nm. The AgNPs had different but prominent effects on either *Citrobacter* sp. A1 or *Enterococcus* sp. C1. At an AgNP concentration of 1000 mg/L, *Citrobacter* sp. A1 retained viability for

* Corresponding author. Block T02, Faculty of Biosciences and Medical Engineering (FBME), Universiti Teknologi Malaysia (UTM), 81310 Skudai, Johor, Malaysia.

E-mail address: nooraini_nar@fbb.utm.my (N.A. Abdul Rashid).

6 hours, while *Enterococcus* sp. C1 retained viability only for 3 hours. *Citrobacter* sp. A1 appeared to be more resistant to AgNPs than *Enterococcus* sp. C1. The cell wall of both strains was found to be morphologically altered at that concentration.

Conclusion: Minute and spherical AgNPs significantly affected the viability of the two bacterial strains selected from the environment. *Enterococcus* sp. C1 was more vulnerable to AgNPs, probably due to its cell wall architecture and the absence of silver resistance-related genes. Copyright © 2015, Taiwan Society of Microbiology. Published by Elsevier Taiwan LLC. This is an open access article under the CC BY-NC-ND license (<http://creativecommons.org/licenses/by-nc-nd/4.0/>).

Introduction

Silver nanoparticles (AgNPs; 1–100 nm in size) are attractive in many industrial applications, especially in the biomedical field,¹ due to their unique physiochemical properties that are different from those of their parental bulk silver. AgNP is an excellent antimicrobial agent due to the well-developed surface and large surface area/volume ratio, which enhance contact with cell surfaces, allowing interaction with certain functional groups.² Various strategies have been developed for the synthesis of AgNPs through manipulation of their size, shape, or surface charge in an effort to improve their antimicrobial property.

There are numerous methods of AgNPs synthesis either through chemical, physical, photochemical, or biological routes.³ Chemical reduction of silver ions in different stabilizers is the most common method for production of stable AgNPs in solution. Additionally, sonochemical (ultrasound) technique has extensively been used to generate novel nanomaterials with unusual properties including silver nanoplates and gold nanorings⁴ and to produce minute silver particles rapidly.⁵

The use of capping agents has been proposed to control the size and shape of AgNPs. Examples of capping agents are polyvinylpyrrolidone (PVP), polyvinylamine, amino alcohols, polyethylene glycol, or sodium dodecyl sulfate, which act as stabilizers preventing AgNPs from forming aggregates or precipitates.⁶ PVP, in particular, is an excellent stabilizer due to its unique chemical and physical properties such as high chemical stability, nontoxicity, and excellent solubility in many polar solvents.^{2,7}

Bulk silver and silver ions have been used as antimicrobial agents for decades.⁸ The current trend of antimicrobial agents focuses on nanosized silver, as it is applied to a wide range of products, including wound dressing, medical devices, clothing, and bedding. AgNPs have been shown to prevent human immunodeficiency virus (HIV) from attaching to the host cells.⁹ In addition, *Aspergillus niger* (fungus), *Staphylococcus* sp., *Bacillus* sp. (Gram-positive bacteria), and *Escherichia coli* (Gram-negative bacteria) have also been reported to be susceptible to AgNPs.⁹ However, the antibacterial mechanism of AgNPs has not been elucidated thoroughly. Thus far, AgNPs are only known to inhibit bacterial growth by cell membrane attachment, penetration, and release into the bacterial cells.¹⁰

Several studies have reported on the antibacterial effects of AgNPs mainly using laboratory strains or clinical pathogens.^{1,8,10,11} It is now known that the release of AgNPs into

the environment increases the contact with the inherent bacteria. Thus, detailed studies are critical to establish the effect of AgNPs on native bacteria. In this study, two environmental bacterial strains, designated as *Citrobacter* sp. A1¹² and *Enterococcus* sp. C1 (from here onward designated as A1 and C1, respectively),¹³ isolated from a sewage oxidation pond in Universiti Teknologi Malaysia (Johor, Malaysia) were used. These bacterial strains have been studied extensively, especially in relations to the biodegradation of several azo dyes.¹⁴ A1 is a Gram-negative coccobacillus from the *Enterobacteriaceae* family. It has the potential to be used in heavy metal reduction, nitrate reduction, sulfate assimilation, quorum sensing, and biofilm formation, making it important in the biodegradation of various xenobiotics and bioremediation of heavy metals.¹² C1, by contrast, is a Gram-positive facultative anaerobic diplococcus, classified as lactic acid bacteria.

To date, this study is possibly the first report on the synthesis of PVP-capped AgNPs by ultrasound-assisted chemical reduction and subsequent determination of their antibacterial activity against *Citrobacter* and *Enterococcus* spp. This is a prerequisite to understand the fate of the microbes in the actual environment upon exposure to AgNPs.

Methods

Chemicals and microorganisms

Chemicals such as AgNO₃ (*Merck KGaA*, Darmstadt, Germany), NaBH₄ (*Sigma-Aldrich*, St Louis, MO, USA), and PVP K15 with a molecular weight of around 10,000 (*Fluka*, Buchs, Switzerland) are of analytical grade. Glutaraldehyde, osmium tetroxide, and sodium cacodylate trihydrate were bought from *Sigma-Aldrich*, while all other chemicals were purchased from *Qrec* (Auckland, New Zealand). The two local bacterial strains A1 and C1, formerly isolated from a sewage oxidation pond, were retrieved from the culture collection of the Nanomaterials Laboratory, FBME, UTM. P5 medium (K₂HPO₄ 35.3 g/L, KH₂PO₄ 20.9 g/L, NH₄Cl 2 g/L, glucose 10 g/L, nutrient broth 20 g/L, and trace elements) was used as the growth medium.¹⁴

Synthesis of AgNPs

The modified ultrasound-assisted chemical reduction method of Goharshadi and Azizi-Toupkanloo¹⁵ was used to

synthesize AgNPs. A solution containing 0.040 g PVP and 0.170 g AgNO₃ in 10 mL was prepared. Ice-cold NaBH₄ (0.038 g in 10 mL) was added dropwise into the PVP-AgNO₃ solution and sonicated for 60 minutes in an ultrasonic bath (Branson 3510; Branson Ultrasonics, Danbury, CT, USA). The sonicated mixture was centrifuged at 13,420 g for 30 minutes, washed thrice with water, and then freeze dried. AgNP powder was redispersed in water using ultrasonication before use.

Characterization of AgNPs

The UV–visible spectrum of the AgNP suspension was acquired spectrophotometrically (Shimadzu UV-1601PC; Shimadzu, Tokyo, Japan) at room temperature. Fourier transform infrared spectrum was measured using a Nicolet IS5-IR spectrometer (Thermo Fisher Scientific, Madison, WI, USA). AgNP powder was mixed with KBr to form a pellet, followed by scanning in the range of 400–4000/cm. The X-ray diffraction (XRD) pattern was recorded over a 2θ range of 30–90° at a scan rate of 1°/min using monochromatic Cu K α radiation ($\lambda = 1.5406 \text{ \AA}$) with an X-ray powder diffractometer (Bruker Advance D8; Bruker AXS, Karlsruhe, Germany). Transmission electron microscopy (TEM) and energy-dispersive X-ray spectroscopy were performed using a transmission electron microscope (JEOL JEM-2100; JEOL, Tokyo, Japan) operating at an acceleration voltage of 200 kV. AgNPs were spiked on a formvar/carbon-coated copper grid and then air dried. The sample was observed at magnification ranging from 25,000 \times to 500,000 \times .

Antibacterial assay

A single colony of A1 or C1 was inoculated separately into fresh 10 mL P5 medium. The culture was incubated overnight at 37°C with shaking at 200 rpm, until OD₆₀₀ reached 1.0 ± 0.2 . Then, the 2 mL overnight culture was centrifuged at 1844 g for 5 minutes; the pellet was washed twice with 0.1M phosphate buffer (PB, pH 7) and resuspended in an equal volume of 0.1 M PB.

A 2-mL bacterial suspension was aliquoted into separate conical flasks containing 100 mL of 0.1 M PB with varying concentrations of AgNPs (10 mg/L, 100 mg/L, and 1000 mg/L), followed by incubation at 30°C with shaking at 200 rpm. Viability of the bacterial cells after exposure was determined hourly and expressed in terms of colony-forming units/mL.

Electron microscopic analysis

Cells treated with 1000 mg/L AgNPs in 0.1 M PB were centrifuged at 295 g for 10 minutes and the pellet was prefixed with 4% (v/v) glutaraldehyde overnight at 4°C. The prefixed cells were washed with 0.1 M cacodylate buffer thrice and postfixed with 1% (v/v) osmium tetroxide for 2 hours at 4°C. The cells were washed thrice with 0.1 M cacodylate buffer and dehydrated in a series of ethanol solutions (35%, 50%, 75%, 95%, and 100%) at 15 minutes each. The fixed cells were dried and gold-coated on scanning electron microscopy (SEM) stub before observation under a scanning electron microscope (JEOL JSM-6390LV; JEOL).

Results

Characterization of synthesized AgNPs

The change in the color of the solution from clear to yellow indicated formation of AgNPs (Figure 1), owing to surface plasmon resonance¹⁶ due to the reduction of Ag⁺ to Ag⁰. A single and narrow surface plasmon resonance absorption band at around 402 nm was observed in the UV–visible spectrum (Figure 2). This finding, which is in good agreement with several studies suggests that this band can be attributed to spherical AgNPs.^{8,17,18}

PVP was chosen for capping and stabilizing AgNPs. Fourier transform infrared spectra corresponding to AgNO₃, PVP, and PVP-capped AgNPs are shown in Figure 3. In the spectrum of PVP, the peak corresponding to the C=O stretching at 1658/cm shifted to 1614/cm with the incorporation of AgNPs in PVP-capped AgNPs. Additionally, the C–N stretching peak shifted from 1070/cm (PVP) to 1061/cm (AgNPs), and the N–OH complex peak, which was at around 1288/cm in the PVP spectrum, was not observed in the AgNP spectrum. These three observations suggest that the AgNPs interacted with PVP, either chemically or physically.^{19,20}

Size, morphology, and crystallinity of the AgNPs were examined using XRD and TEM, while the composition of the nanoparticles was analyzed by energy-dispersive X-ray spectroscopy. Figure 4A shows the XRD diffraction pattern of the synthesized AgNPs. Five broad diffraction peaks observed at 38.1°, 44.3°, 64.4°, 77.5°, and 81.5° were indexed as (111), (200), (220), (311), and (222) planes, respectively. The result matches the Joint Committee on Powder Diffraction Standards (JCPDS) database (file no. 04-9783), indicating that the AgNPs correspond to face-centered cubic silver (Figure 4B). The broadening of the diffraction peak implies that the AgNPs formed are minute particles.¹⁵ TEM images of the AgNPs and the histogram for particle size distribution are shown in Figure 5, exhibiting particles that are spherical in shape, in the nanosize range (<65 nm), and widely dispersed. The particle size was primarily in the range of 2–20 nm, with an average of 15.60 nm. Small-sized AgNPs are useful in many applications²¹ and potentially possess greater antibacterial activity.^{8,22} The TEM image also shows that the AgNPs are covered with a layer of PVP (Figure 5B). Interplanar spacing of synthesized AgNPs is around 0.23 nm, as seen in the TEM

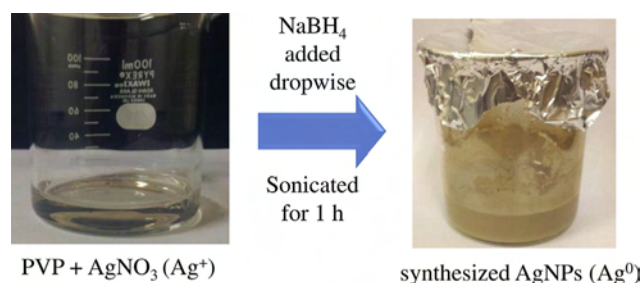


Figure 1. Change in the color of PVP-AgNO₃ solution from clear to yellow, indicating a reduction of Ag⁺ to Ag⁰ during synthesis of AgNPs. AgNP = silver nanoparticle; PVP = polyvinylpyrrolidone.

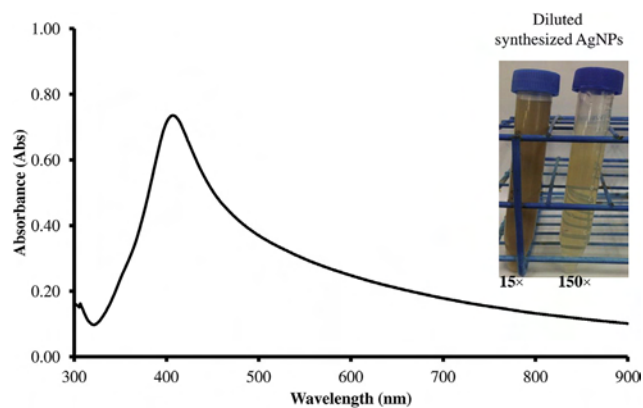


Figure 2. UV–visible spectrum of synthesized AgNPs (150× dilution; inset: the diluted AgNP suspension). AgNP = silver nanoparticle.

image (Figure 5C). The energy-dispersive X-ray spectroscopy spectrum shows the presence of major peaks at 0.3 keV and 3 keV, confirming the presence of PVP and silver in the AgNPs (Figure 6).

Determination of toxicity of AgNPs on A1 and C1

Antibacterial effect of AgNPs

Toxicity of AgNPs toward the model bacterial strains was investigated according to exposure time and concentration. Various concentrations of AgNPs, including 0 mg/L, 10 mg/L, 100 mg/L, and 1000 mg/L, were considered. Bacterial viability of both A1 and C1 decreased as the concentration of AgNPs increased (Figure 7).

Gram-negative A1 survived in 0.1M PB with 10 mg/L and 100 mg/L AgNPs after 24 hours of incubation (Figure 7A), while C1 lost viability after 10 hours of incubation at these concentrations (Figure 7B). Despite its resilience, at the AgNP concentration of 1000 mg/L, A1 lost its viability after

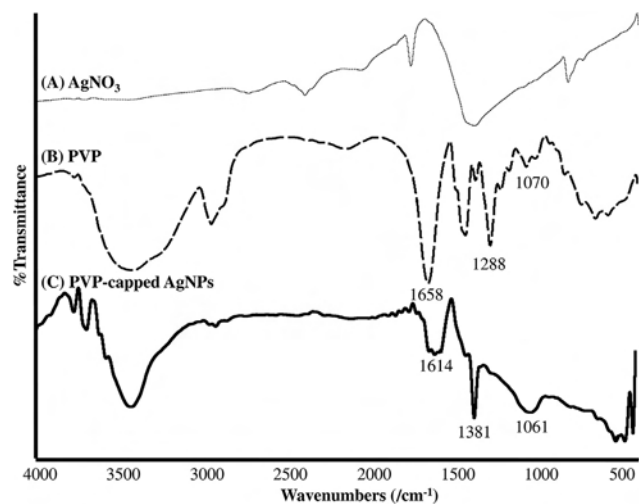


Figure 3. FTIR spectra of (A) AgNO_3 , (B) PVP, and (C) AgNPs in the presence of PVP. AgNP = silver nanoparticle; FTIR = Fourier transform infrared; PVP = polyvinylpyrrolidone.

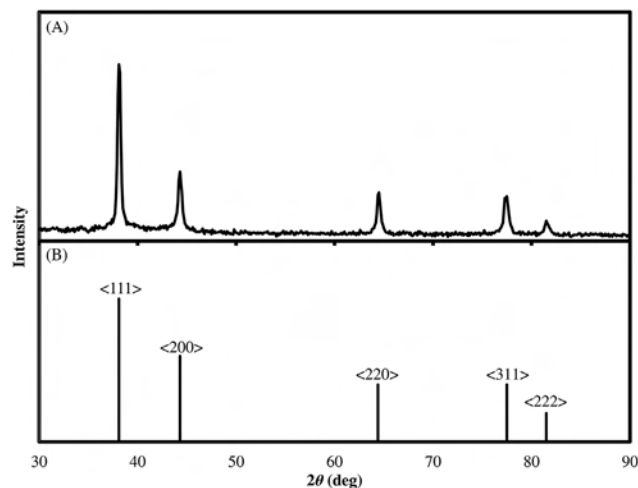


Figure 4. XRD pattern of (A) AgNPs and (B) pure silver with FCC symmetry (JCPDS file no. 04-0783). AgNP = silver nanoparticle; FCC = face-centered cubic; JCPDS = Joint Committee on Powder Diffraction Standards; XRD = X-ray diffraction.

6 hours, whereas 3-hour incubation was sufficient for complete loss of viability of C1. These results indicate that C1 is more susceptible to AgNPs than A1.

Effect of AgNPs on bacterial cell morphology

Significant morphological changes were observed for the two strains, as examined under SEM, after treatment with 1000 mg/L AgNPs (Figure 8). Observation was made following exposure of A1 to AgNPs for 6 hours and of C1 for 3 hours. Both strains were found to have uneven cell surface, suggesting cell lysis (Figures 8B and 8D). Irregularly shaped particles are possibly aggregated AgNPs that adhere to bacterial cells, or perhaps cellular debris.

Discussion

AgNPs may be discharged into the environment during production and disposal of products containing AgNPs.²³ The discharged AgNPs are likely to accumulate in the aquatic environment leading to contamination, which impair the function of useful microorganisms in the environment. *Pseudomonas chlororaphis* O6 (a soil bacterium beneficial to plants) has been reported to lose its culturability due to AgNPs.¹¹

The appearance of surface plasmon resonance peak in the UV–visible spectrum of the AgNPs can be associated with their nanoparticle size, shape, and interparticle interactions and the effects of the surrounding medium on the nanoparticles.²¹ The spectrum indicates that AgNPs are dispersed in nanosize range and are spherical in shape. This was then confirmed with TEM image and XRD patterns.

The efficacy of AgNPs as antibacterial agent depends mainly on their size.^{8,22–25} In this study, AgNPs mostly in the range of 2–20 nm, with an average size of 15.6 nm, were synthesized. Smaller particles were assumed to be easily internalized by microorganisms through the peptidoglycan and plasma membranes into cytoplasm due to less spatial hindrance.^{8,22} The antibacterial activity of AgNPs is partly due to the release of Ag^+ from the AgNPs in aqueous

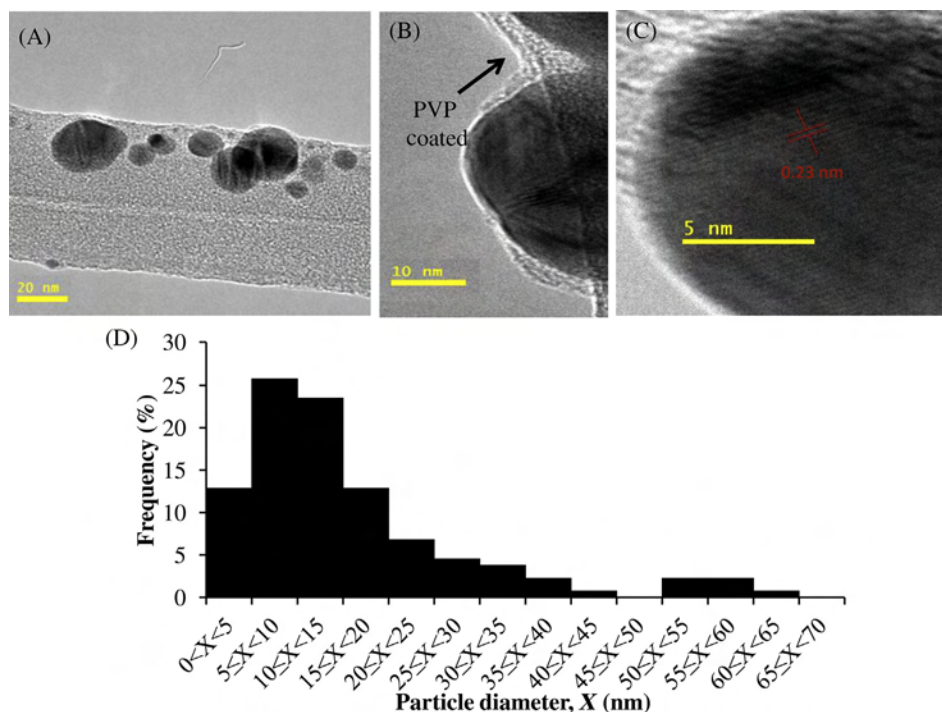


Figure 5. TEM images of AgNPs: (A) at 100,000 \times magnification, (B) at 250,000 \times magnification, and (C) at 500,000 \times magnification, and (D) histogram of particle size distribution. AgNP = silver nanoparticle; PVP = polyvinylpyrrolidone; TEM = transmission electron microscopy.

solution.²² Smaller AgNPs provide greater surface area, which can rapidly release Ag^+ via oxidation^{22,25} and increase the generation of reactive oxidative species (ROS).²³ It has been reported that AgNPs of about 15 nm in size generated more ROS than bigger particles (30 nm and 50 nm), and the ROS are capable of destroying the cell membrane, DNA, and mitochondria, resulting in cell death.²³

PVP-capped AgNPs are known to possess excellent stability toward environmental change (including pH change or ionic strength), making them desirable in the industries.¹

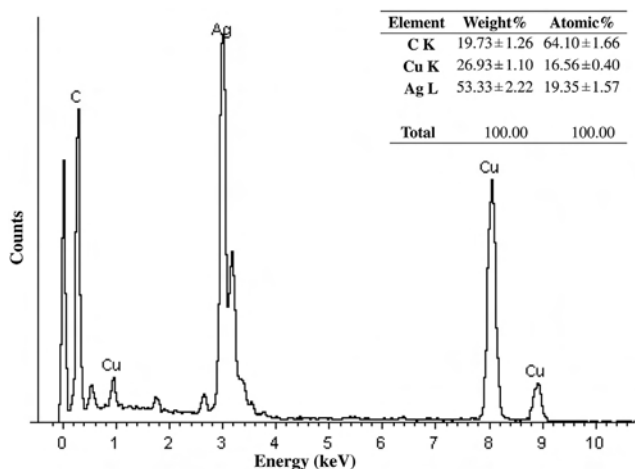


Figure 6. Elemental analysis of AgNPs using EDX. AgNP = silver nanoparticle; EDX = energy-dispersive X-ray spectroscopy.

The toxicity of AgNPs is dependent not only on the particle size, but also on the surface charge of the capping agent.²⁶ PVP-capped AgNPs have increased the tendency of cell-particle interaction, resulting in higher toxicity, compared to uncoated H_2 -AgNPs, citrate-coated AgNPs, and branched polyethyleneimine-coated AgNPs.²⁶ Thus, PVP has been selected as the stabilizer for AgNP synthesis.

There are three possible mechanisms of PVP adsorption onto the nanoparticles: (1) interaction with O atoms only; (2) interaction with N atoms only; or (3) interaction with both N and O atoms.²⁷ Figure 3 indicates that the shift of the Fourier transform infrared band can be associated with the coordination between PVP with AgNPs, suggesting that the coordination is possibly via N and O atoms. For particle size <50 nm, the N atom in PVP coordinated with silver, forming a protective layer due to the electronegativity of N, which is lower than that of O.²⁰ Nonetheless, both N and O are coordinated with silver when steric effect is strengthened with the increase in diameter of the AgNPs.²⁰

The antibacterial effect of AgNPs on A1 and C1 was first investigated in rich media: P5 medium and nutrient broth. Preliminary studies showed that PVP-capped AgNPs did not affect the viability of A1 and C1 in rich media (data not shown), probably due to the agglomeration of AgNPs upon interaction with the organic components from the rich media²⁴ or due to the bacterial-specific defense mechanism against AgNPs in nutrient-rich media.²⁸ Therefore, it has been rationalized that for subsequent investigations, toxicity studies of AgNPs should be conducted in PB.

It has been demonstrated that PVP-capped AgNPs completely inhibited the viability of A1 and C1 at 1000 mg/L. As a comparison, *E. coli* and *Bacillus subtilis* completely

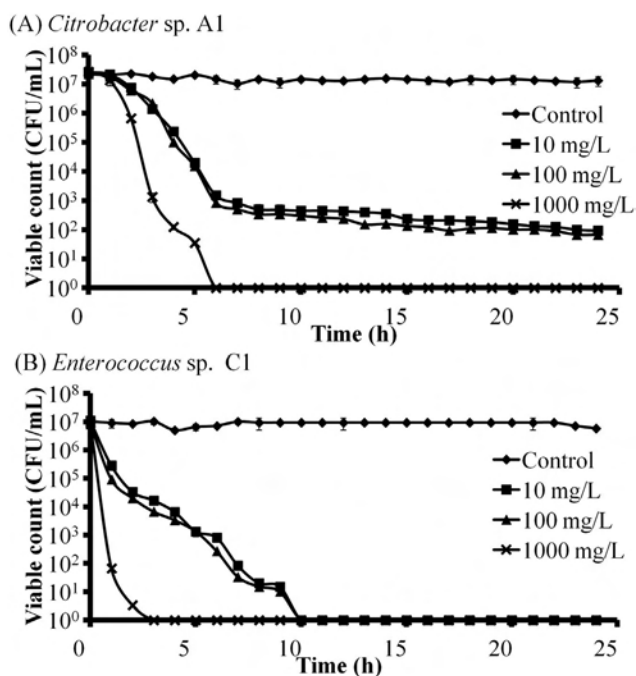


Figure 7. Antibacterial effect of AgNPs at concentrations 10–1000 mg/L on (A) *Citrobacter sp. A1* and (B) *Enterococcus sp. C1* in 0.1M PB (pH 7) at 30°C with shaking at 200 rpm. AgNP = silver nanoparticle; CFU = colony-forming unit; PB = phosphate buffer.

lost viability after 3 hours of exposure to 1.6 mg/L AgNPs in phosphate buffered saline.²⁹ In another study, the growth of AgNP-treated *Staphylococcus aureus* and *E. coli* were inhibited at 50 mg/L, while *S. aureus* and *E. coli* cells treated with 100 mg/L AgNPs in Mueller–Hinton broth lost viability after 4 hours and 3 hours of exposure, respectively.³⁰ This concentration (at 1000 mg/L of PVP-capped AgNPs) is relatively high compared to that used in other studies. This is possibly due to the bacterial resistance, as it has been suggested that these two strains possess genes that encode metal ion transporters, and metal-binding or heavy metal detoxification proteins.^{12,13}

Resistance level to AgNPs was found to vary between the two strains. This can be associated with the difference in cell wall architecture; A1, being Gram negative, was probably more resistant to AgNPs than the Gram-positive C1. *E. coli* and *Shewanella oneidensis* have been reported to be more tolerant toward AgNPs compared to *B. subtilis*, owing to the lipopolysaccharide layer in the outer membrane of these Gram-negative bacteria.³¹ Hence, the lipopolysaccharide layer of A1 may trap and block AgNPs from entering the cell, as also reported by Lara et al.¹⁰

Bacterial genotype also plays an important role in the defense against AgNPs, as well as against Ag⁺. Several strains of bacteria possess genes that encode oxidative stress protection proteins, damage repair proteins, and metal efflux pumps, and are involved in the production of extracellular polymeric substances, resulting in a better bacterial adaptation and defense against silver.³² For example, the presence of *silB* gene in *Salmonella* serotypes

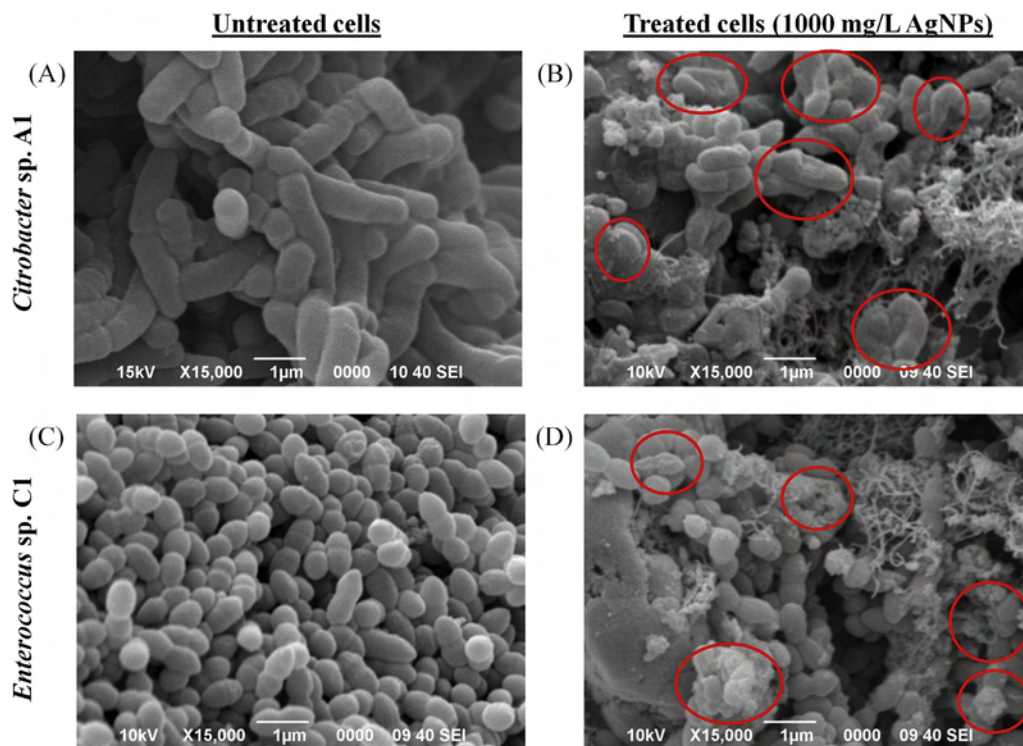


Figure 8. SEM images showing the effect of AgNPs on bacterial cell morphology: (A) untreated *Citrobacter sp. A1*; (B) *Citrobacter sp. A1* treated with 1000 mg/L AgNPs in 0.1M PB at 30°C with shaking at 200 rpm for 6 hours; (C) untreated *Enterococcus sp. C1*; and (D) *Enterococcus sp. C1* treated with 1000 mg/L AgNPs in 0.1M PB at 30°C with shaking at 200 rpm for 3 hours (red circles indicate morphological change of the cell). AgNP = silver nanoparticle; PB = phosphate buffer; SEM = scanning electron microscope.

assists in its resistance against Ag^+ , Hg^{2+} , and tellurite, as well as against several antibiotics.³³ Gram-negative bacteria can also transport Cu^+ across the outer membrane to protect the periplasm from copper-induced damage using Cus efflux system.³⁴ The system is also involved in silver detoxification in *E. coli*.³⁵

P-type ATPases and cation diffusion facilitators may also be involved in metal resistance, by exporting metal ions from the cytoplasm to the periplasm, followed by pumping of the metal ion out of the cell.³³ P-type ATPases are coded by *copA* gene, which is involved in copper efflux; *copA* may be involved in mediating the efflux of silver, since deletion of the gene resulted in hypersensitivity of *E. coli* K-12 and O157:H7 chromosomes to silver, as well as to copper.³⁶ The previously published draft genome sequence for A1 showed that the bacterium possesses genes for inner membrane cation protein (SilA), silver binding protein (SilE), transcriptional regulatory proteins (SilR), copper/silver efflux system proteins (CusCBA), and sensor/responder system proteins (CusRS).¹² These proteins are commonly reported in silver- and copper-tolerant bacteria.^{23,32,36,37} Nevertheless, genes coding for these proteins were not identified in the draft genome sequence of C1.¹³ The lack of these genes in C1 probably contributes to its slightly higher sensitivity to silver as compared to A1.

SEM images suggest physical damages of the AgNPs-treated bacterial cells, when compared to untreated cells (Figure 8). Cell damage may be due to direct attachment of AgNPs to the cell wall and cell membrane of the bacteria, followed by penetration into the cell. AgNPs preferentially target bacterial membrane, thus weakening the cell wall, resulting in dissipation of the proton motive force.^{11,38} Accumulation of AgNPs in the cell wall increases cell permeability through disruption of the cell membrane, inducing cell death. Another possible antimicrobial strategy is the high affinity of silver towards sulfur and phosphorus.³⁹ Thiol-containing proteins and enzymes interact with AgNPs or Ag^+ , causing deactivation. Ag^+ can inactivate DNA replication by reacting with the phosphorus moieties in the DNA.³⁹ AgNPs and Ag^+ have also been suggested to interact electrostatically with the negative charge in the cell wall, inducing free radicals, in particular ROS.⁴⁰

In conclusion, spherical PVP-capped AgNPs (~15 nm in size) have been synthesized successfully. The synthesized AgNPs significantly affect the viability of the two environmental isolates A1 and C1. C1 is more susceptible to AgNPs, as it is Gram positive and does not seem to possess silver-resistance-related genes. Thus, it can be concluded that AgNPs released into the environment, upon accumulation, may have significant impact on the native microorganisms and the ecosystem.

Conflicts of interest

The authors declare no competing interest.

Acknowledgments

This research was financially supported by the Ministry of Science, Technology and Innovation (MOSTI) through

TechnoFund Grant, Nanotechnology National Directorate (Vot R.J130000.7925.4H009).

References

1. Kora AJ, Rastogi L. Enhancement of antibacterial activity of capped silver nanoparticles in combination with antibiotics, on model gram-negative and gram-positive bacteria. *Bioinorg Chem Appl* 2013;2013:871097.
2. Bryaskova R, Pencheva D, Nikolov S, Kantardjiew T. Synthesis and comparative study on the antimicrobial activity of hybrid materials based on silver nanoparticles (AgNps) stabilized by polyvinylpyrrolidone (PVP). *J Chem Biol* 2011;4:185–91.
3. Tran QH, Nguyen VQ, Le AT. Silver nanoparticles: synthesis, properties, toxicology, applications and perspectives. *Adv Nat Sci Nanosci Nanotechnol* 2013;4:1–20.
4. Jiang LP, Xu S, Zhu JM, Zhang JR, Zhu JJ, Chen HY. Ultrasonic-assisted synthesis of monodisperse single-crystalline silver nanoplates and gold nanorings. *Inorg Chem* 2004;43:5877–83.
5. Fujimoto T, Terauchi SY, Umehara H, Kojima I, Henderson W. Sonochemical preparation of single-dispersion metal nanoparticles from metal salts. *Chem Mater* 2001;13:1057–60.
6. Mahtig B, Tatlis B, Fahmi A, Haase H. Dendrimer stabilized silver particles for the antimicrobial finishing of textiles. *J Text I* 2013;104:1042–8.
7. Washio I, Xiong Y, Yin Y, Xia Y. Reduction by the end groups of poly(vinyl pyrrolidone): a new and versatile route to the kinetically controlled synthesis of Ag triangular nanoplates. *Adv Mater* 2006;18:1745–9.
8. Chudasama B, Vala AK, Andhariya N, Mehta RV, Upadhyay RV. Highly bacterial resistant silver nanoparticles: synthesis and antibacterial activities. *J Nanopart Res* 2010;12:1677–85.
9. Jaidev LR, Narasimha G. Fungal mediated biosynthesis of silver nanoparticles, characterization and antimicrobial activity. *Colloid Surf B* 2010;81:430–3.
10. Lara HH, Ayala-Núñez NV, Turrent LdCl, Padilla CR. Bacterial effect of silver nanoparticles against multidrug-resistant bacteria. *World J Microbiol Biotechnol* 2010;26:615–21.
11. Dimkpa CO, Calder A, Gajjar P, Merugu S, Huang W, Britt DW, et al. Interaction of silver nanoparticles with an environmentally beneficial bacterium, *Pseudomonas chlororaphis*. *J Hazard Mater* 2011;188:428–35.
12. Chan GF, Gan HM, Rashid NAA. Genome sequence of *Citrobacter* sp. strain A1, a dye-degrading bacterium. *J Bacteriol* 2012;194:5485–6.
13. Chan GF, Gan HM, Rashid NAA. Genome sequence of *Enterococcus* sp. strain C1, an azo dye decolorizer. *J Bacteriol* 2012;194:5716–7.
14. Chan GF, Rashid NAA, Chua LS, Ab. I. N. Nasiri R, Ikubar MRM. Communal microaerophilic-aerobic biodegradation of Amaranth by novel NAR-2 bacterial consortium. *Bioresour Technol* 2012;105:48–59.
15. Goharshadi EK, Azizi-Toupkanloo H. Silver colloid nanoparticles: ultrasound-assisted synthesis, electrical and rheological properties. *Powder Technol* 2013;237:97–101.
16. Burda C, Chen X, Narayanan R, El-Sayed MA. Chemistry and properties of nanocrystals of different shapes. *Chem Rev* 2005;105:1025–102.
17. Naghavi K, Saion E, Rezaee K, Yunus WMM. Influence of dose on particle size of colloidal silver nanoparticles synthesized by gamma radiation. *Radiat Phys Chem* 2010;79:1203–8.
18. Lee CJ, Karim MR, Casudevan T, Kim HJ, Raushan K, Jung MJ, et al. A comparison method of silver nanoparticles prepared by the gamma irradiation and *in situ* reduction methods. *Bull Korean Chem Soc* 2010;31:1993–6.

19. Hong HK, Park CK, Gong MS. Preparation of Ag/PVP nanocomposites as a solid precursor for silver nanocolloids solution. *Bull Korean Chem Soc* 2010;**31**:1252–6.
20. Wang H, Qiao X, Chen J, Wang X, Ding S. Mechanisms of PVP in the preparation of silver nanoparticles. *Mater Chem Phys* 2005;**94**:449–53.
21. Desai R, Mankad V, Gupta SK, Jha PK. Size distribution of silver nanoparticles: UV–visible spectroscopic assessment. *Nanosci Nanotechnol Lett* 2012;**4**:30–4.
22. Pelgrift RY, Friedman AJ. Nanotechnology as a therapeutic tool to combat microbial resistance. *Adv Drug Deliv Rev* 2013;**65**: 1803–15.
23. Marambio-Jones C, Hoek EMV. A review of the antibacterial effects of silver nanomaterials and potential implications for human health and the environment. *J Nanopart Res* 2010;**12**: 1531–51.
24. Gnanadhas DP, Thomas MB, Thomas R, Raichur AM, Chakravorttya D. Interaction of silver nanoparticles with serum proteins affects their antimicrobial activity *in vivo*. *Antimicrob Agents Chemother* 2013;**57**:4945–55.
25. Allen HJ, Impellitteri CA, Macke DA, Heckman JL, Poynton HC, Lazorchak JM, et al. Effects from filtration, capping agents, and presence/absence of food on the toxicity of silver nanoparticles to *Daphnia magna*. *Environ Toxicol Chem* 2010;**29**: 2742–50.
26. El Badawy AM, Silva RG, Morris B, Scheckel KG, Suidan MT, Tolaymat TM. Surface charge-dependent toxicity of silver nanoparticles. *Environ Sci Technol* 2011;**45**:283–7.
27. Mdluli PS, Sosibo NM, Mashazi PN, Nyokong T, Tshikhudo RT, Skepu A, et al. Selective adsorption of PVP on the surface of silver nanoparticles: a molecular dynamics study. *J Mol Struct* 2011;**1004**:131–7.
28. Khan SS, Kumar EB, Mukherjee A, Chandrasekaran N. Bacterial tolerance to silver nanoparticles (SNPs): *Aeromonas punctata* isolated from sewage environment. *J Basic Microb* 2011;**51**: 183–90.
29. Lee S, Lee J, Kim K, Sim SJ, Gu MB, Yi J, et al. Eco-toxicity of commercial silver nanopowders to bacterial and yeast strains. *Biotechnol Bioproc E* 2009;**14**:490–5.
30. Kim SH, Lee HS, Ryu DS, Choi SJ, Lee DS. Antibacterial activity of silver-nanoparticles against *Staphylococcus aureus* and *Escherichia coli*. *Korean J Microbiol Biotechnol* 2011;**39**: 77–85.
31. Suresh AK, Pelletier DA, Wang W, Moon J-W, Gu B, Mortensen NP, et al. Silver nanocrystallites: biofabrication using *Shewanella oneidensis*, and an evaluation of their comparative toxicity on gram-negative and gram-positive bacteria. *Environ Sci Technol* 2010;**44**:5210–5.
32. Xiu Z, Liu Y, Mathieu J, Wang J, Zhu D, Alvarez PJJ. Elucidating the genetic basis for *Escherichia coli* defense against silver toxicity using mutant arrays. *Environ Toxicol Chem* 2014;**9999**: 1–5.
33. Losasso C, Belluco S, Cibin V, Zavagnin P, Mičetić I, Gallochio F, et al. Antibacterial activity of silver nanoparticles: sensitivity of different *Salmonella serovars*. *Front Microbiol* 2014;**5**:1–9.
34. Rensing C, Grass G. *Escherichia coli* mechanisms of copper homeostasis in a changing environment. *FEMS Microbiol Rev* 2003;**27**:197–213.
35. Franke S, Grass G, Nies DH. The product of the *ybdE* gene of the *Escherichia coli* chromosome is involved in detoxification of silver ions. *Microbiology* 2001;**147**:965–72.
36. Gupta A, Phung LT, Taylor DE, Silver S. Diversity of silver resistance genes in IncH incompatibility group plasmids. *Microbiology* 2001;**147**:3393–402.
37. Silver S. Bacterial silver resistance: molecular biology and uses and misuses of silver compounds. *FEMS Microbiol Rev* 2003;**27**: 341–53.
38. Sondi I, Salopek-Sondi B. Silver nanoparticles as antimicrobial agent: a case study on *E. coli* as a model for Gram-negative bacteria. *J Colloid Interface Sci* 2004;**275**:177–82.
39. Ravishankar RV, Jamuna BA. Nanoparticles and their potential application as antimicrobials. In: Méndez-Vilas A, editor. *Science against microbial pathogens: communicating current research and technological advances*. Spain: Formatex Research Center; 2011. p. 197–209.
40. Hajipour MJ, Fromm KM, Ashkarran AA, Jimenez de Aberasturi D, de Larramendi IR, Rojo T, et al. Antibacterial properties of nanoparticles. *Trends Biotechnol* 2012;**30**: 499–511.